Aggregation of a Surfactant Squaraine in Langmuir–Blodgett Films, Solids, and Solution

Huijuan Chen,† William G. Herkstroeter,† Jerome Perlstein,† Kock-Yee Law,*,‡ and David G. Whitten*,†

Center for Photoinduced Charge Transfer, University of Rochester, Hutchison Hall, Rochester, New York 14627

Received: January 31, 1994®

The aggregation of a surfactant squaraine, 4-(*N*-methyl-*N*-(carboxypropyl)amino)phenyl-4′-(*N*,*N*-dibutylamino)-phenylsquaraine (SBA), has been studied in a variety of media, including organic solvents, aqueous cyclodextrin (CD) solutions, vesicles, monolayers, Langmuir–Blodgett films, and pure solid dye films. As a monomer in organic solvent, SBA exhibits sharp and intense absorption with λ_{max} ranging from 622 to 656 nm and fluorescence emission at λ_F 637–678 nm. In dilute aqueous solution the monomer absorbs at 650 nm and gives a fluorescence at 678 nm. The dimer absorbs at 594 nm and is nonfluorescent. This structural assignment is supported by studying the spectroscopic properties of SBA in CD solutions. SBA forms 1:1 inclusion complexes with α- and β-CD which absorb at $\lambda_{max} \sim 650$ nm and emit at $\lambda_F \sim 672$ nm with a fluorescence quantum yield a factor of 2–3 higher than that in pure water. The inclusion of the squaraine chromophore in α- and β-CD is also indicated by ^{1}H NMR spectral data which suggest that the squaraine chromophore is in a relatively nonpolar environment. In γ-CD solution, due to the larger cavity size (9.5 Å vs 5.7 and 7.8 Å in α- and β-CD, respectively), a 2:1 complex between SBA and γ-CD is formed. This 2:1 complex which essentially is the dimer of SBA absorbs at 594 nm and does not fluoresce. A further blue-shift in absorption, λ_{max} at 500–540 nm, is observed when SBA is incorporated in vesicles (at high concentrations), monolayers, supported LB films, and pure solid dye film. From available crystal structure data and the compression isotherm data in this study, it is calculated that SBA adopts either a translation layer or a glide layer structure in these aggregates. Interestingly, the intermolecular interaction between the squaraine chromophores in these aggregates is shown to be similar to that in microcrystals of bis(4-methoxyphenyl)squaraine, which also shows blue-shifted absorption in the aggregated state relative to the monomer.

Introduction

Squaraine dyes with their novel "cyclobutadiene quinone" structure and sharp strong transitions far into the visible spectrum have been widely used in a number of applications including their incorporation into solid-state electrophotographic devices.[1] An interesting feature of squaraine dyes is their very strong fluorescence when dispersed as a monomer in solution[2] and contrasting lack of fluorescence in the aggregated or solid state. Nonetheless, studies from our laboratories and other groups indicate that the nonluminescent aggregates or microcrystallites can be photochemically or photoelectrochemically active in a number of cases.[3,4] The observation that several squaraines can exist in different aggregated forms[5-7] or different types of crystals,[8] which may in turn exhibit different photogeneration efficiencies, suggests that intermolecular interactions in the crystal or aggregate may play a major role in determining the photogeneration mechanism and efficiency.

We have been interested in the aggregation and its subsequent effect on the photoconductivity of squaraines for some time. Crystal structures for a number of squaraines having *p*-phenyl substituents have been determined along with their absorption spectral properties. X-ray structural data indicate that bis(4-methoxyphenyl)squaraine exhibits a translational layer structure in which stacks of squaraine molecules are in a near "card-pack" array. The interplanar distance is ~3.5 Å, and the major interaction is through the C–O dipole.[9,10] The absorption of the microcrystal is blue-shifted relative to the solution monomer absorption. Another type of molecular arrangement for squaraines was reported by Wingard,[11] who showed that bis(2-methyl-4-dimethylaminophenyl)squaraine adopts a slipped stack arrangement with major intermolecular interaction arising from charge transfer between the anilino ring and the central four-membered ring.[11] The solid-state absorption of bis(2-methyl-4-dimethylaminophenyl)squaraine is broad and red-shifted relative to the solution absorption. Very similar structural and optical absorption data were also reported for bis(2-hydroxy-4-diethylaminophenyl)-squaraine.[12] A number of recent elegant studies by Kamat and collaborators have demonstrated that aggregation and complex formation can play a major role in determining the luminescence properties of hydroxy-substituted squaraines; in several cases acid–base equilibria and hydrogen-bonding effects play major roles in determining both the aggregate structure as well as the photophysical behavior.[7,13,14]

In order to provide a bridge between solution and solid-state properties, we have designed, synthesized, and studied a functionalized squaraine, 4-(*N*-methyl-*N*-(carboxypropyl)amino)-phenyl-4′-(*N*,*N*-dibutylamino)phenylsquaraine (SBA), which contains a simple squaraine chromophore embedded within an amphiphilic structure.

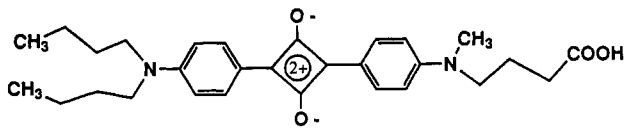

SBA

It was predicted that this molecule could be readily incorporated into Langmuir–Blodgett films at the air water interface and supported multilayers but that it should possess sufficient solubility to be studied in aqueous and mixed aqueous–organic solutions. In our studies we find that SBA can be readily incorporated into a wide variety of media under conditions where forms ranging

† Department of Chemistry, University of Rochester, Rochester, NY 14627.
‡ Xerox Corporation, Webster Research Center, 800 Phillips Road, 114-39D, Webster, NY 14580.
* To whom correspondence should be addressed.
® Abstract published in *Advance ACS Abstracts,* April 15, 1994.

0022-3654/94/2098-5138$04.50/0

from extended aggregate to dimer to monomer can be prepared and investigated. In the present paper we report results of these investigations which begin to provide a systematic picture of the aggregation process and the connection between aggregate structure and photophysics.

Experimental Section

Materials. *N,N*-Dibutylaniline (97%), *N*-methylaniline (99+%), ethyl 4-bromobutyrate (95%), 3,4-dihydroxy-3-cyclobutene-1,2-dione (98%), thionyl chloride (99%), α-, β-, and γ-cyclodextrins, cadmium chloride (99.99%)), sodium bicarbonate (99%), and potassium phosphate (monobasic and dibasic, 99%) were purchased from Aldrich. L-α-Dimyristoylphosphatidylcholine (99+%) was purchased from Sigma and tributyl orthoformate from Pfaltz & Bauer. Diethyl ether (anhydrous), *N,N*-dimethylformamide, 2-propanol, methanol, ethyl acetate, hexane, methylene chloride, chloroform, dimethyl sulfoxide, and concentrated hydrochloric acid were Certified Grade from Fisher. All solvents for spectroscopic studies were Spectroscopic Grade from Fisher. The spreading solvent for monolayer work was pentene-stabilized HPLC Grade chloroform from Fisher. Suitable water was obtained by passing purified in-house distilled water through a Millipore-RO/UF water purification system. All other materials were used as received.

Deuterated solvents and reagents, DMSO-d_6, $CDCl_3$, NaOD, DCl, and D_2O were purchased from MSD Isotopes. Transparent tin oxide glass slides were purchased from Delta Technologies.

General Techniques. Melting points were taken on a Mel-Temp melting point apparatus and are uncorrected. Infrared spectra were determined on a Matheson Galaxy 6020 FTIR. Proton NMR spectra were recorded on a General Electric/Nicolet QE300 MHz spectrometer. Mass spectra were measured on a Varian VG 7035 mass spectrometer, and FAB mass spectra were measured at the Midwest Center of Mass Spectrometry. Elemental analyses were carried out at Galbraith Laboratories. Absorption spectra for both solution and solid-state studies were recorded on an IBM 9430 spectrophotometer. Absorption spectra for monolayers at the air–water interface were recorded in situ with a homemade spectrometer equipped with optical fibers and a multichannel diode array detector.[15] Fluorescence spectra were recorded on a SPEX Fluorolog-2 spectrofluorometer and are uncorrected. The circular dichroism study was carried out on a JASCO J-40 spectropolarimeter. Potassium phosphate solutions (10 mM, both monobasic and dibasic) were used to adjust the pH to 7.5 in aqueous solution studies. The pH values were measured with an Orion Research digital ionalyzer/501 pH meter.

Monolayers of SBA were prepared by spreading a chloroform solution of SBA ($\sim 10^{-4}$ M) onto an aqueous subphase, which contained cadmium chloride (2.5×10^{-4} M) and potassium bicarbonate (3×10^{-5} M, pH = 6) on a KSV 5000 film balance at room temperature (~20 °C). Precleaned[16] hydrophilic glass and tin oxide glass substrates were used in this work. Bilayer vesicles were prepared according to the procedure of Hope et al.[17] at a pH of 5.0 in a Cell Disrupter W220F from Heat Systems-Ultrasonics, Inc.

^{1}H-NMR studies of the dye/cyclodextrin solutions were performed on a 500-MHz Varian VXR-500S spectrometer. The pH value (pD 7.5) of the NMR sample in D_2O was adjusted with NaOD/DCl solutions in D_2O.

Photoelectrochemical experiments on the SBA-modified SnO_2 electrodes were carried out on an in-house assembled apparatus consisting of an Electrochemical Analyzer, Model BAS100B from Bioanalytical Systems, and a xenon arc lamp system (Model A1010) from Photon Technology International Inc. The details of the apparatus and the measuring procedures have been reported earlier.[3]

Synthesis of *N*-Methyl-*N*-(carboxypropyl)aniline. *N*-Methyl-*N*-(carboxypropyl)aniline was prepared according to the procedure described by Desai[18] by reacting for about 16 h 0.14 mmol (15.0 g) of *N*-methylaniline and 0.14 mmol (27.3 g) of ethyl 4-bromobutyrate at ~110 °C in the presence of 11.9 g of sodium acetate and 0.12 g of iodine. The reaction mixture was then cooled to room temperature. The crude product was dissolved in water and then made basic with sodium hydroxide; it was then extracted with ether. The combined extract was washed with water, dried over $MgSO_4$, evaporated to remove solvent, and isolated by vacuum distillation. Pure *N*-methyl-*N*-(ethyl 4-butanoate)aniline was isolated as a clear liquid. Yield 24.6 g (79.5%): bp 116–118 °C at 0.25 mmHg; ^{1}H-NMR ($CDCl_3$) δ 7.25 (t, 2H), 6.75 (m, 3H), 4.16 (q, 2H), 3.40 (t, 2H), 2.96 (s, 3H), 2.38 (t, 2H), 1.94 (m, 2H) and 1.28 (t, 3H).

The ester product (10 g, 45 mmol) was then hydrolyzed in 150 mL of 5% KOH at reflux for 2 h. After cooling, the reaction mixture was washed with ether (2 × 70 mL). The aqueous layer was then adjusted to pH 5.5 with concentrated hydrochloric acid, extracted with ether (3 × 100 mL), dried over $MgSO_4$, and evaporated to remove solvent. *N*-Methyl-*N*-(carboxypropyl)-aniline was obtained as an oily liquid with a yield of 8.5 g (97.4%): bp 147–150 °C/0.2 mmHg dec.; ^{1}H-NMR ($CDCl_3$) δ 7.26 (t, 2H), 6.75 (m, 3H), 3.40 (t, 2H), 2.96 (s, 3H), 2.45 (t, 2H) and 1.95 (m, 2H).

Synthesis of 1-Chloro-2-(*p*-dibutylaminophenyl)cyclobutene-3,4-dione. 1-Chloro-2-(*p*-dibutylaminophenyl)cyclobutene-3,4-dione was synthesized according to the procedure described by Wendling et al.[19] A slight modification of the procedure was made in this work. Typically, a solution containing 1,2-dichlorocyclobutene-3,4-dione (4.5 g, 30 mmol, freshly prepared according to the procedure of De Selms and co-workers[20]) and *N,N*-dibutylaniline (6.1 g, 30 mmol) in 80 mL of methylene chloride was added dropwise to a methylene chloride solution of the catalyst (5.3 g, 40 mmol of $AlCl_3$ in 30 mL of CH_2Cl_2) at reflux. After the addition, the mixture was refluxed for an additional hour. The product solution was poured into 80 mL of ice water containing 2 drops of concentrated HCl. The organic layer was separated, washed with water, dried over $MgSO_4$, filtered, and evaporated. The pure produce (3.3 g) was obtained as light-yellow crystals by column chromatography on silica gel (70–230 mesh), with ethyl acetate/hexane = 1:9 as eluent. Yield: 34.7%; mp 74.0–75.0 °C; IR (KBr) 1797 cm^{-1}, 1603 cm^{-1}, 1570 cm^{-1}; ^{1}H-NMR ($CDCl_3$) δ 8.11 (d, 2H), 6.72 (d, 2H), 3.40 (t, 4H), 1.62 (m, 4H), 1.40 (m, 4H) and 0.95 (t, 6H); UV–visible λ_{max} ($CHCl_3$) 416 nm. Mass obsd m/z = 319.85 (M^+). Mass calcd for $C_{18}H_{22}O_2NCl$ 319.83.

Synthesis of 1-(*p*-Dibutylaminophenyl)-2-hydroxycyclobutene-3,4-dione. 1-Chloro-2-(*p*-dibutylaminophenyl)cyclobutene-3,4-dione (1.0 g, 3.13 mmol) was suspended in 50 mL of 18% HCl solution. The mixture was brought to reflux for about 2.5 h and was cooled to room temperature. The top organic layer, a yellow liquid, was decanted into a round bottom flask. After evaporation of the solvent, a brown residue was obtained. The brown solid was washed with water (3 × 20 mL) and was recrystallized from a mixture of DMSO (~3 mL) and water (20 mL). A light-yellow solid was isolated by filtration, washed with methylene chloride (3 × 5 mL), and vacuum dried at 60 °C overnight: yield 1-(*p*-dibutylaminophenyl)-2-hydroxycyclobutene-3,4-dione 0.84 g (90%); mp 243–244 °C (dec.); IR (KBr) 1767 cm^{-1}, 1578 cm^{-1}; ^{1}H-NMR (DMSO-d_6) δ 7.83 (d, 2H), 6.80 (d, 2H), 3.38 (t, 4H), 1.48 (m, 4H), 1.27 (m, 4H), 0.87 (t, 6H). FAB mass obsd m/z = 302.1758 (M + H). Mass calcd for $C_{18}H_{24}O_3N$ 302.1756.

Synthesis of 4-(*N*-Methyl-*N*-(carboxypropyl)amino)phenyl-4′-(*N,N*-dibutylamino)phenylsquaraine (SBA). SBA was synthesized by a condensation reaction as described in the literature.[21] *N*-Methyl-*N*-(carboxypropyl)aniline (0.53 g, 2.76 mmol), 2-propanol (25 mL), and tributyl orthoformate (2 mL) were placed in a 3-neck 100-mL flask equipped with a magnetic stirbar. The mixture was stirred and brought reflux under a nitrogen

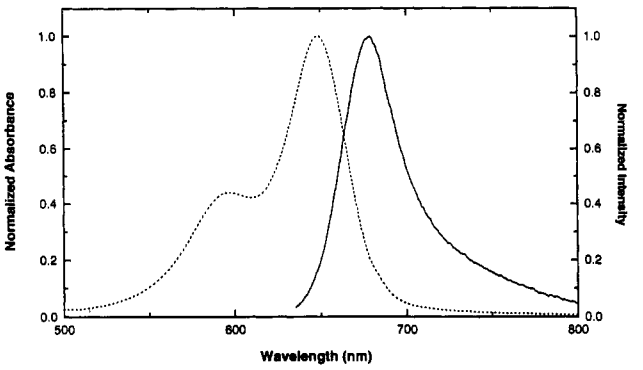

Figure 1. Absorption and fluorescence emission spectra of SBA in H_2O ([SBA] = 3×10^{-6} M, pH = 7.5, (- - -) absorption and (—) fluorescence).

atmosphere. A solution containing 1-(*p*-dibutylaminophenyl)-2-hydroxycyclobutene-3,4-dione (0.41 g, 1.38 mmol) in ~2 mL of DMSO was added slowly through a pressure-equalizing funnel over a 3-h period. After the addition was complet, the product mixture was refluxed for 3 h. A blue precipitate was isolated by filtration. After washing with 2-propanol and ether, the blue solid was vacuum dried and was purified by recrystallization from $DMSO/CH_2Cl_2$. Yield: 0.33 g (50%); mp 213.0–214.0 °C (dec.); ^{1}H-NMR δ 8.09–8.06 (dd, 4H), 6.96–6.94 (dd, 4H), 3.50 (m, 6H), 3.16 (s, 3H), 2.28 (t, 2H), 1.79 (m, 2H), 1.60–1.55 (m, 4H), 1.32 (m, 4H) and 0.90 (t, 6H); IR (KBr) 1587 cm^{-1}, 1735 cm^{-1}; UV–visible λ_{max} ($CHCl_3$) 633 nm, $\epsilon_{max} = 3.10 \times 10^5$ M^{-1} cm^{-1}. FAB mass obsd m/z = 477.2753 (M + H). Mass calcd for $C_{29}H_{37}O_4N_2$ 477.2753. Anal calcd: C 72.91, H, 7.81, N, 5.87, O 13.41. Found: C 72.83, H 7.74, N 5.82, O 13.61.

Results

Solution Properties of SBA. SBA is readily soluble in organic solvents such as chloroform, methanol, and dimethyl sulfoxide to give blue solutions with sharp, strong absorption maxima as well as intense fluorescence. In chloroform, for example, the absorption maximum lies at 632 nm with an extinction coefficient of 3.1×10^5 M^{-1} cm^{-1}; the fluorescence maximum lies at 653 nm and the fluorescence lifetime is 2.5 ns. These values (Table 1) are typical for squaraine dyes in dispersed, monomeric form. The aqueous solubility of SBA is pH dependent. From pH 5 to 6, the range that matches the pH of the aqueous subphase used in preparing Langmuir–Blodgett films, insolubility prevails. SBA is, however, both stable and sufficiently soluble in water at a pH of 7.5 for spectroscopic investigations. As shown in Figure 1, the aqueous absorption spectrum of SBA shows a maximum at 650 nm with a shoulder at 594 nm. Dilute aqueous solutions of SBA also fluoresce with a maximum at 678 nm. The excitation spectrum monitored at this wavelength corresponds only to the 650-nm absorption. Higher concentrations of SBA in water increase the peak at 594 nm relative to the 650-nm maximum. Assigning the former to the H-dimer of SBA and the latter to the monomer, the spectral changes with concentration of SBA can be described quantitatively by the equilibrium of eq 1 with an equilibrium constant of 4.0×10^4 M^{-1} at 24.5 °C.

$$2\text{SBA} \rightleftarrows \text{SBA}_2 \qquad (1)$$

The monomer–dimer equilibrium constant K_1 corresponds to a ΔG_0 = –6.29 kcal/mol; measurement of the temperature dependence of K_1 from 20 to 50 °C indicates that ΔH_0 = –6.84 kcal/mol and ΔS_0 = –1.83 cal/mol deg. These values are similar or slightly smaller in magnitude (corresponding to a smaller K) than those measured for other large aromatic molecules including porphyrins and cyanine dyes.[22] The blue shift in absorption concurrent with dimerization is also consistent with an H-dimer or card pack association such as has been observed in crystals of some previously investigated squaraines as well as in aqueous solutions of certain cyanine and oxazine dyes.[9,10,23]

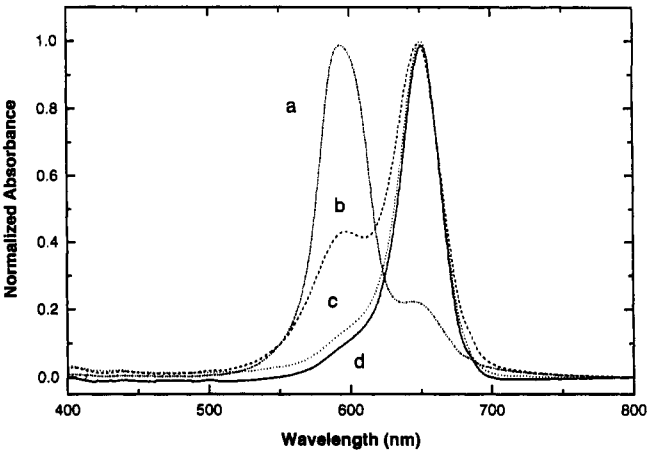

Figure 2. Absorption spectra of SBA (3×10^{-6} M) in aqueous solutions: (a) in γ-cyclodextrin (1×10^{-3} M); (b) in H_2O; (c) in β-cyclodextrin (2×10^{-3} M); (d) in α-cyclodextrin (1×10^{-2} M).

TABLE 1: Absorption and Relative Fluorescence Emission Data of SBA in Different Solutions

solvent	λ_{max} (nm)	λ_F (nm)	quantum yield[a]
benzene	634	648	1.00
ether	622	637	0.88
$CHCl_3$	632	653	0.70
DMSO	656	678	0.24
MeOH	642	667	0.099
H_2O	650[c]	678	0.097
α-CD (r = 1:1000)[b]	650	673	0.20
β-CD (r = 1:500)[b]	650	673	0.29
γ-CD (r = 1:500)[b]	594[c]	672	0.0025

[a] Relative value, assume the quantum yield is 1.0 in benzene. [b] r = [SBA]/[cyclodextrin], [dye] = 2.0×10^{-6} M. [c] The absorption maximum of the dominant peak.

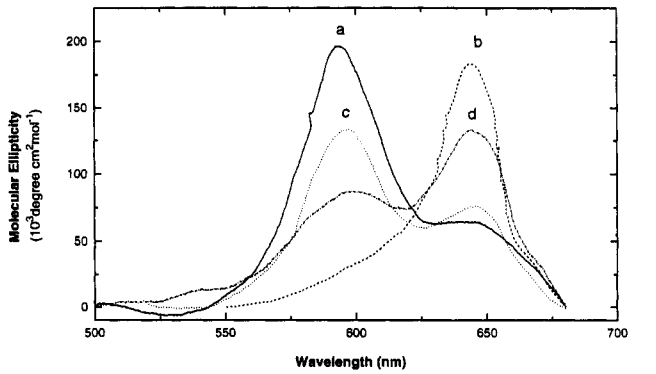

Figure 3. Circular dichroism spectra of SBA (3×10^{-6} M) in aqueous cyclodextrin solutions: (a) γ-CD (1.25×10^{-3} M); (b) β-CD (2.5×10^{-3} M); (c) γ-CD/β-CD = 5×10^{-4} M/8×10^{-4} M; (d) γ-CD/β-CD = 5×10^{-4} M/1.25×10^{-3} M.

The aqueous solubility of SBA can be significantly increased by the presence of α-, β-, or γ-cyclodextrin. As shown in Figure 2, both α- and β-cyclodextrin increase the intensity of the 650-nm absorption peak, whereas γ-cyclodextrin enhances the 594-nm peak at the expense of the longer wavelength peak. Strong fluorescence is observed from the α- and β-cyclodextrin solutions (Table 1), while only weak fluorescence can be detected in the γ-cyclodextrin solutions.

As shown in Figure 3, cyclodextrin solutions of SBA show in each case a strong circular dichroism that corresponds to spectroscopic absorption with a positive value for the molecular ellipticity. The results indicate that SBA forms inclusion complexes with cyclodextrins in aqueous solution.[24]

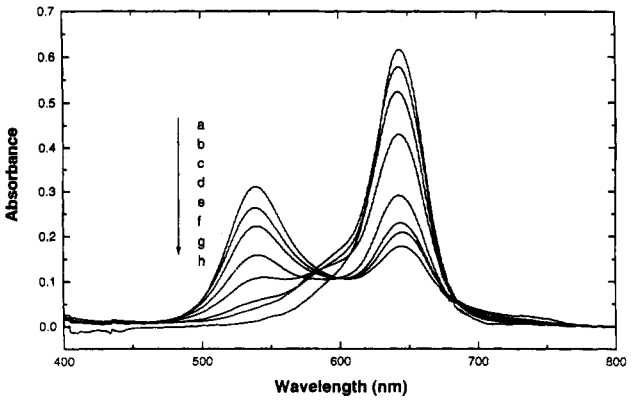

Figure 4. Absorption spectra of SBA [4.5×10^{-6} M] in DMPC vesicles. DMPC/SBA = (a) 4/1; (b) 6/1; (c) 8/1; (d) 10/1; (e) 15/1; (f) 25/1; (g) 30/1; (h) 50/1.

TABLE 2: ^{1}H NMR Data of SBA in Various Media

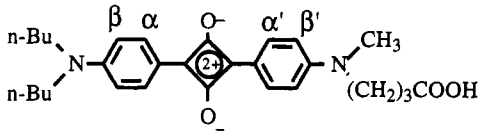

solvent	$\delta = \delta(H_\alpha) - \delta(H_\beta)$ (ppm)
D_2O	1.070
DMSO	1.148
$CDCl_3$	1.583
γ-CD/D_2O	1.337
β-CD/D_2O	1.220

^{1}H NMR spectra of squaraines in D_2O and a range of organic solvents exhibit substantial solvent sensitivity, most strikingly apparent by a comparison of the differences in chemical shifts for the α and β aromatic protons. In earlier studies, variation in these chemical shift differences had been attributed to interactions of solvent molecules with the squaraine chromophore.[25] Table 2 lists these difference values for SBA in $CDCl_3$, DMSO, D_2O, and aqueous cyclodextrin solutions. The chemical shift differences for both the β- and γ-cyclodextrin solutions of SBA are consistent with having the squaraine chromophore in the cyclodextrin inclusion complexes in relatively nonpolar surroundings.[25]

The solubility of SBA in water is also enhanced by addition of the phospholipid, dimyristoylphosphatidylcholine (DMPC), which readily forms bilayer vesicles (liposomes) in aqueous solution with a reported phase transition (melting) temperature of 24.0 °C. When the ratio of DMPC to SBA is high (>50), the absorption spectrum of SBA is dominated by the 650-nm transition. As the ratio [DMPC]/[SBA] decreases (Figure 4) the transition at 594 nm can be detected as a shoulder, but subsequent decreases lead to a broader transition even more blue-shifted (540 nm) than that attributed to the dimer. The fluorescence intensity at 657 nm decreases as the ratio [DMPC]/[SBA] decreases, and no new fluorescence is observed as the spectrum shifts. Due to the gradual changes of the absorption spectra as the ratio [DMPC]/[SBA] decreases, it is not possible to treat the equilibria involved here quantitatively.

Langmuir–Blodgett Films of SBA at the Air–Water Interface. Pure SBA forms a stable monolayer film when spread from an evaporating chloroform solution over water at pH 5–6. The surface pressure–area isotherm is shown in Figure 5a; the collapse pressure is ca. 40 mN/m while a limiting area of 38 Å^2/molecule is indicated. The early maximum in the isotherm at a molecular area of 55 Å^2 disappears as films are decompressed and then subsequently recompressed; the hysteresis behavior of the films is indicated in Figure 5b. The films at the air–water interface show absorption dominated by transitions near 500–530 nm which shift slightly to the red as the surface pressure is increased (Figure 6). The strong blue shift in the absorption is similar to that observed at very high [SBA]/[DMPC] ratios in aqueous phospholipid solutions and in the transferred multilayers or solid films of SBA (vide infra) but quite different from those transitions assigned above to monomer and dimer in solution. It is noteworthy that the blue-shifted spectrum is observed even at very low surface pressures (2 mN/m) where little "forced" packing of the chromophores is anticipated. Only very weak fluorescence with λ_{max} near 650 nm is observed from the films at the air–water interface. This fluorescence occurs very close to that attributed to monomer (vide supra) and is ascribed to a residual amount of monomer not incorporated in the predominant aggregated species.

Langmuir–Blodgett Multilayers and Other Solid Films of SBA. The compressed films of SBA at the air–water interface can be readily transferred to solid supports such as glass, quartz, or optically transparent tin oxide electrodes to form supported multilayers. Transfer ratios are close to unity, and multilayer assemblies containing up to 11 layers of pure SBA can be easily prepared with good reproducibility. Figure 7 shows the absorption spectra of freshly prepared and heated LB assemblies of SBA (four layers); the initially prepared multilayer assemblies show a relatively sharp transition at 532 nm, and there is no detectable fluorescence. Based on spectral similarities, it seems reasonable to ascribe the predominant species in the multilayers to an aggregate similar in structure to those observed in the films at the air–water interface and in the phospholipid vesicles at high [SBA]/[host phospholipid] ratios. Mixed films and supported layers could be prepared from SBA using stearic acid as a diluent. Dilution up to a 1:10 or 1:20 [SBA]/[stearic acid] mole ratio results in only a small decrease in the absorption at 532 nm and little increase in the monomer. Thus, the tendency for SBA to associate to form aggregates is quite strong in the LB films and assemblies.

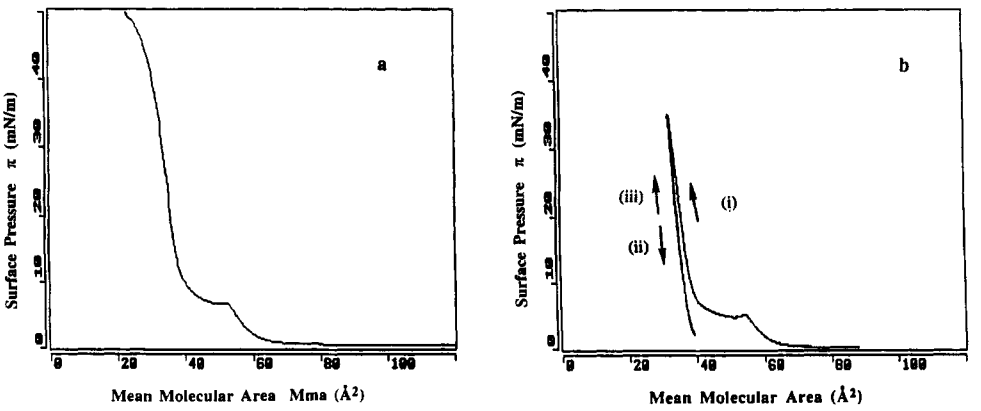

Figure 5. Surface pressure–area isotherms of SBA monolayers: (a) normal isotherm, compressed once; (b) hysteresis behavior, three sweeps between 2 and 35 mN/m; (i) first compression; (ii) decompression; (iii) second compression.

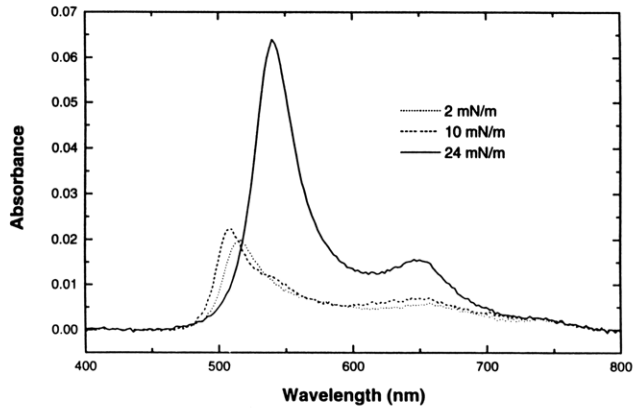

Figure 6. Absorption spectra of SBA monolayers at air–water interface.

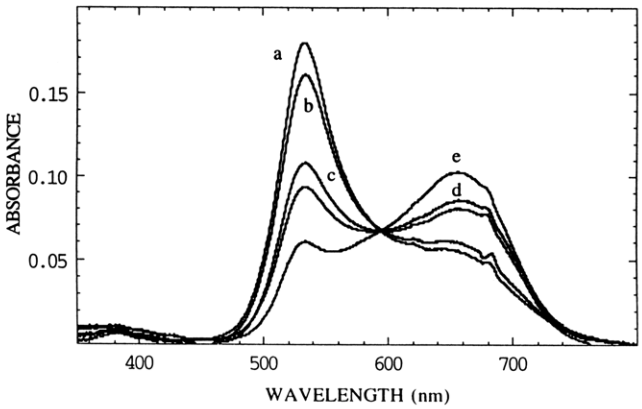

Figure 7. Absorption spectra of a four-layer LB film of SBA: (a) as prepared; (b–e) film in (a) heated at 110 °C for 10, 30, 45, and 110 min, respectively.

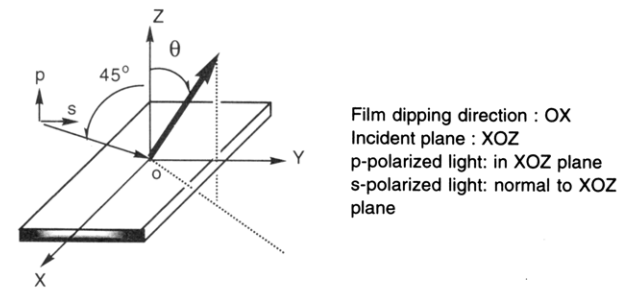

Figure 8. Polarized absorption study of SBA LB films.

As shown in Figure 7, the freshly prepared assemblies of pure SBA showing the blue-shifted spectrum can be converted to a new species by heating at 110 °C over a period of less than 2 h. The conversion is evidently quite clean as indicated by the isosbestic point; the product can be dissolved from the assembly by washing with $CHCl_3$ to give a solution of undecomposed SBA. The new species absorbs at ~655 nm, slightly to the red of the monomer in solution. In contrast to the monomer, however, this species shows no fluorescence. LB assemblies of SBA deposited on an optically transparent SnO_2 electrode show the blue-shifted absorption (530 nm) described above and show similar photoelectrochemical activity to those recently described for tetraalkylsquaraines.[3] Irradiation of a modified SnO_2 electrode consisting of a single monolayer of SBA at 530 nm in a conventional photoelectrochemical cell results in a 200–250-nA cathodic photocurrent. The action spectrum obtained matches quite closely the absorption spectrum of the blue-shifted aggregate shown in Figure 7. No photocurrent was observed upon irradiation of the red-shifted species obtained by heating.

The supported LB assemblies of SBA were also investigated in terms of preferential absorption of p- and s-linear polarized light to gain an indication of the chromophore orientation within the assembly.[26] As shown in Figure 8, supported single-layer (one side only coated) assemblies of pure SBA on quartz were examined. In the case of uniaxial orientation of the transition moment with a tilt angle ϕ (the tilt angle of the transition moment of the dye chromophore with respect to the surface normal), the absorption intensity ratio A_p/A_s is given by eq 2, where the four-phase system is composed of (1) the incident air phase (index of refraction, $n_1 = 1.00$), (2) the SBA-LB film (n_2 assumed to be 1.50), (3) the quartz substrate ($n_3 = 1.54$), and (4) the final phase of air. The term $i = 45°$, while r, the angle of refraction at the LB film–substrate interface, can be calculated from the relationship $n_1 \sin(i) = n_3 \sin(r)$.[27]

$$\frac{A_p}{A} = \frac{n_1 \cos(i) + n_3 \cos(r)}{\cos(r) + n_3 \cos(i)}\left(\cos i \cos r + \frac{2n_1^3 n_3 \sin^2 i}{n_2^4 \tan^2 \phi}\right) \quad (2)$$

The result of the calculation using the measured values gives $\phi = 50 \pm 2°$ with good reproducibility. Since the direction of the transition dipole moment of the squaraine chromophore can be assigned as being along the long axis,[12] this measurement indicates that the squaraine chromophore in SBA tends to tilt considerably from the surface normal in the blue-shifted (freshly prepared) aggregates. When slides containing the blue-shifted aggregate were heated, the aggregate spectra shifted to the red as illustrated in Figure 7. Analyses based on absorption of p- and s-polarized light to determine the tilt angle gave 47° at 534 nm but 60° at the heat-shifted maximum at 650 nm. This calculation takes into account the reflection of incident light from the air–film and film-substrate interfaces; however, it makes the questionable assumption that the system is uniaxial. Another factor which could introduce error is the value for n_2, the refractive index of the LB film; we chose the value 1.50 which is that for a fatty acid LB assembly.[28] Finally, in cases such as the heated film where there can be overlapping peaks, the ratio given in eq 2 may not be precisely evaluated.

SBA can also be spread in thin films by evaporation on a clean glass surface from solvents such as aqueous methanol or dry chloroform. In each case, the films show spectra similar to those obtained from the freshly prepared LB assemblies with predominance of the "aggregate" peak at 530 nm.

Discussion

From the results presented above, it can be seen that SBA exists as several different species, depending upon its state and the medium in which it is hosted. The water-soluble forms of SBA described earlier are readily identified as monomer and dimer. The ability to alter dye solubilities and to shift equilibria among dye monomer and dimer makes cyclodextrin inclusion complexation particularly important when working with aqueous solutions of organic dye molecules.[29] Consequently, such inclusion complexation can affect those spectroscopic characteristics and photophysical properties influenced by the state of dye aggregation such as electronic absorption spectra and fluorescence quantum yields.[29,30] Addition of α- or β-cyclodextrin to aqueous SBA solutions clearly results in conversion of the dispersed dye monomer to a cyclodextrin-incorporated monomer, whereas addition of γ-cyclodextrin affects the conversion of the monomer to a cyclodextrin-incorporated dimer. Using the limiting area of 38 Å^2/molecule calculated from the pressure–area isotherm of SBA (Figure 5) as a rough indication of the size of SBA (the vertically oriented squaraine chromophore is estimated to occupy ca. 25 Å^2/molecule while the measured 38 Å^2 corresponds approximately to the cross sectional area of two linear hydrocarbon chains), we estimate that incorporation of no more than a single molecule of SBA in the cavities of α- and β-cyclodextrin (diameters 5.7 and 7.8 Å, respectively) should be possible. For γ-cyclodextrin, the larger radius (9.5 Å) indicates the cavity might be large enough to incorporate two squaraine chromophores; indeed, in several previous studies molecules of similar estimated size have been found to be incorporated in γ-cyclodextrin as dimers.[30,31]

SCHEME 1: Equilibria for SBA and Cyclodextrins in Aqueous Solutions

SBA in α-CD/γ-CD/H_2O System

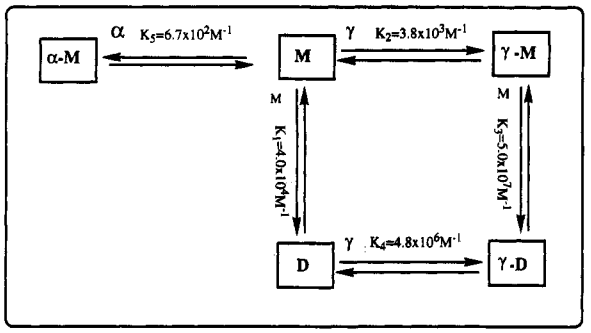

SBA in β-CD/γ-CD/H_2O System

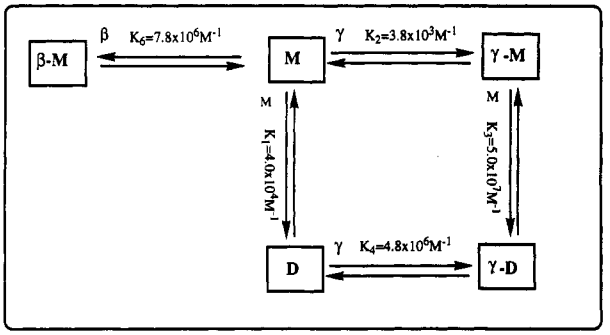

Although the absorption maxima for solutions of cyclodextrin-incorporated SBA are similar to those obtained for SBA in aqueous solution, the ^1H NMR chemical shift differences between the α and β phenyl protons (Table 2) are consistent with a nonpolar environment for the squaraine chromophore.[25] The strong induced circular dichroism (ICD) observed is also consistent with incorporation of the squaraine into the cyclodextrin cavity in each case;[24] the positive value for the molecular ellipticity in the ICD spectra indicates quite reasonably that the transition dipole moment (long axis aligned) for the incorporated squaraine has a relatively small angle of inclination ($\theta < 54.7°$) with the symmetry (z) axis of the cyclodextrin cavity.[32]

Using the measured equilibrium constant K_1 together with a quantitative investigation of the competition between the different cyclodextrins for SBA, it is possible to evaluate the various equilibria present as outlined in Scheme 1.[23] Measurement of these equilibrium constants requires measurement of individual absorption spectra of the monomer and dimer of SBA. The monomer absorption spectrum can be readily measured at low SBA concentrations in water or in the presence of either α- or β-cyclodextrin; it is assumed that the SBA monomer spectrum is independent of its host medium. Determination of the dimer spectrum is complicated because complete conversion to dimer in either the presence or the absence of γ-cyclodextrin is not possible. Even under the most favorable conditions where equilibria are shifted to maximize the formation of the dimer, residual monomeric species still contribute measurably to the overall absorption spectrum. Appropriate corrections must be applied to such a spectrum to establish the spectrum of the dimer alone. Proper size matching between the guest and the hosts cavity leads to substantially larger equilibrium constants. Not surprisingly, the binding constant for SBA in α-cyclodextrin is much smaller than that for the 1:1 SBA:β-cyclodextrin complex.[33] The relatively strong preference of γ-cyclodextrin to incorporate SBA as a dimer is quantitatively indicated by a comparison of K_2, K_3, and K_4. A relatively constrained environment for the squaraine chromophore of SBA in the cyclodextrin cavity is also indicated by the increase in both fluorescence lifetime and quantum efficiency in β-cyclodextrin compared to the monomer in pure water. However, for the dimer incorporated in γ-cyclodextrin, no fluorescence is detected and the lifetime of the excited state formed (followed by recovery of the bleached transient at ≈594 nm) is indicated to be very short (95 ± 15 ps).[34]

The behavior of SBA in aqueous phospholipid (DMPC) solution has not been extensively investigated, but the results obtained thus far suggest that the presumed incorporation of SBA into a bilayer structure provides a bridge between the properties in fluid solution and in solid films or crystals. At low SBA/DMPC ratios, the absorption spectrum is dominated largely by the transition associated with monomeric squaraine. The absorption is sharp, and moderately strong fluorescence is observed. As the SBA/DMPC ratio increases the dimer becomes discernible, and upon further increase a shift to the blue with a final maximum close to that observed for the LB films and supported multilayers is observed. The lack of isosbestic points as the SBA/DMPC mole ratio is increased (in contrast to those observed for other aggregates currently under investigation)[35] suggests that the association to form dimer and presumably aggregate of increasingly higher order is a continuous process in which there is no distinct energy minimum associated with a specific aggregate size. The dominance of the "limiting aggregate transition" at ca. 540 nm when the SBA/DMPC ratio reaches 1/6 suggests that even if totally mixed phospholipid–SBA vesicles exist under these conditions they must consist of large zones of nearly pure squaraine in an extended aggregate structure very similar to that in the LB films.

The very strong tendency for SBA to form dimers or higher aggregates either at the air–water interface, in aqueous solution, in phospholipid bilayers, in γ-cyclodextrin solutions, or in evaporated solids suggests a unique structure with some long-range ordering. At the air–water interface, the specific environment imposes the requirement that the hydrophilic groups all point in the same direction limiting the layer packing to one of two most probable types: either (a) a translation layer in which all molecules are identical and related by simple translations or (b) a perpendicular glide layer which contains a glide plane symmetry element perpendicular to the water (or support) surface. Other possibilities include a simple trigonal layer or hexagonal layer or layers with more than one molecule in the asymmetric unit. However, besides occurring very infrequently the absence of any discrete exciton splittings in the absorption spectra would suggest these layers as being unlikely candidates for the packing arrangement.

Monte Carlo cooling methods for determining the apparent global and nearby local minima structures for a translational layer assembly of molecules have been developed by one of us,[36] and a similar methodology can be applied for predicting the packing modes of the glide layer. The method makes use of Kitaigorodskiis Aufbau principle (KAP), in which the layer structure is built up in three substructural stages, each stage representing a local energy minimum: stage 0, a single molecule; stage 1, a packing of molecules to form a one-dimensional stack; and finally stage 2, a packing of stacks to form the two-dimensional monolayer. Complete details for the construction and determination of the local minima of each stage have been presented previously.[37,38] Here we present details pertinent only to SBA.

For the "single molecule stage 0", bond lengths and bond angles were obtained from previous X-ray studies on squaraines and fatty acids. Pieces of structures from the bis(4-methoxyphenyl)-squaraine, the bis(2-hydroxy-4-diethylaminophenyl)squaraine (reference codes MXPBUQ, and VAYSET of the Cambridge Structural Database[39]), hexatriacontane (HXTACM), and stearic acid (STARAC) were connected to form a rough SBA structure. Bond lengths were then optimized using CHEM-X's level 1 optimizer which allows for bond length optimization while keeping

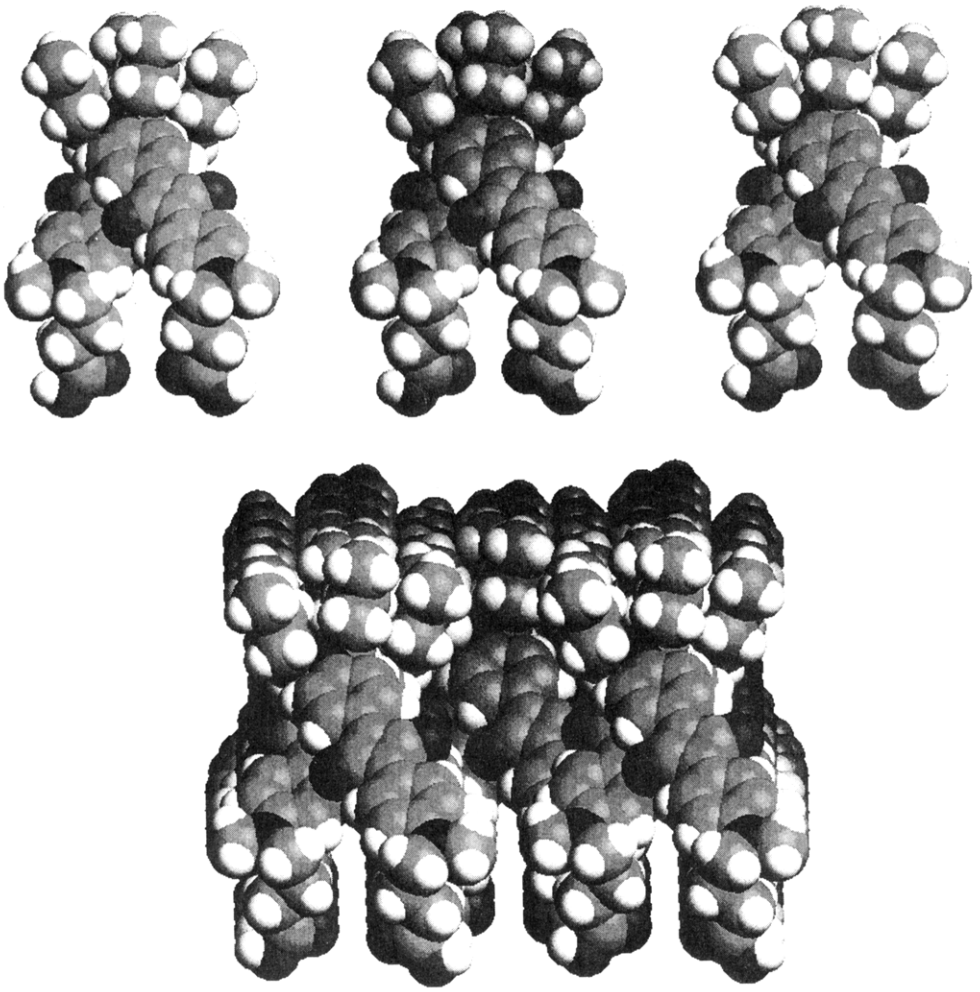

Figure 9. Monte Carlo simulation results for the first local minimum of the perpendicular glide layer. The top view is a cross section of the three identical glide chains that come together to make the perpendicular glide layer. The view is looking down the 9.90-Å glide axis (*b*-axis) showing the overlap of the two molecules which make up the "glide dimer". The bottom view is a cross section of the glide layer slightly tilted to show the top hydrophobic surface. The 7.5-Å *a*-axis points to the right and the 9.90-Å *b*-axis points into the figure. The hydrophilic region is at the bottom of the figure. Note the compact nature of the hydrophobic chains versus the more open structure with cavities between the hydrophilic groups.

all bond angles fixed.[40] The result is a single conformation for SBA in a local energy minimum used for STAGE 1 computations.

Monte Carlo cooling was applied to a collection of five stage 0 molecules to determine the apparent global energy and nearby local energy minima for the translation and glide aggregates (stage 1). The force field used was the nonbonded atom–atom potential and torsion terms taken from MM2 of Allinger[41] with MM2 parameters from MACROMODEL[42] plus an electrostatic term using Gasteiger partial charges on each atom[43] and a linear distance-dependent dielectric constant. Details of the force field and parameters used are described elsewhere.[36-38] Rotations about the single bonds (13 in all, excluding rotation about the hydroxy bond attached to carbon) were included in each Monte Carlo step. Within 10 kcal of the global minimum, 42 unique local minima were found for the translation aggregate and 73 unique minima for the glide aggregate. Each of these was then used in stage 2 of KAP to obtain the final monolayer geometries of SBA.

Monte Carlo cooling was applied to each of the stage 1 minima. Three stacks were used to construct the layers. The translation stacks come together to form the translation layer structure, and the glide stacks come together to form the perpendicular glide layer structure. The random variables for the translation layer have been described previously.[36] In the case of the glide layer, the resulting unit cell must have an enclosed angle between the repeat vectors of 90° and the glide planes on each stack must be parallel to one another and perpendicular to the water surface. Consequently, there is only 1 degree of freedom associated with the formation of this layer, namely, lateral translation of the stacks. As in stage 1, the internal degrees of freedom associated with single bond rotations were included in each Monte Carlo step. The resulting global and apparent local minima for each layer type are shown in Table 3. Of the 700 local minima collected, only 3 unique layers within 5 kcal of the global minimum were found for the translation layer and 14 for the glide layer (only the first 6 including the global are shown in the table). Table 3 also gives predicted cell dimensions, surface area/molecule, the

TABLE 3: Apparent Global and Local Minima Structures for SBA Monolayers

	unit cell dimensions[a]					
rank order	*a*	*b*	γ	surface area[b]	tilt angle[c]	ΔE[d]
			Translation Layers			
0 (global)	8.92	4.90	102.7	42.59	40.17	0
1	8.56	5.07	100.3	42.74	45.73	0.49
2	9.83	4.56	101.5	43.95	30.57	4.07
			Glide Layers			
0 (global)	7.40	9.32	90.00	34.50	46.64	0
1	7.50	9.90	90.00	37.14	53.53	0.01
2	13.03	7.97	90.00	51.94	64.09	0.42
3	12.05	8.08	90.00	48.67	63.51	0.78
4	9.60	9.05	90.00	43.43	44.56	2.63
5	15.12	7.67	90.00	58.00	64.22	2.76

[a] Unit cell in angstroms, γ in degrees. [b] Surface area/molecule in Å^2. [c] Tilt of transition moment with respect to surface normal. [d] Energy in kcal of local minima above the global.

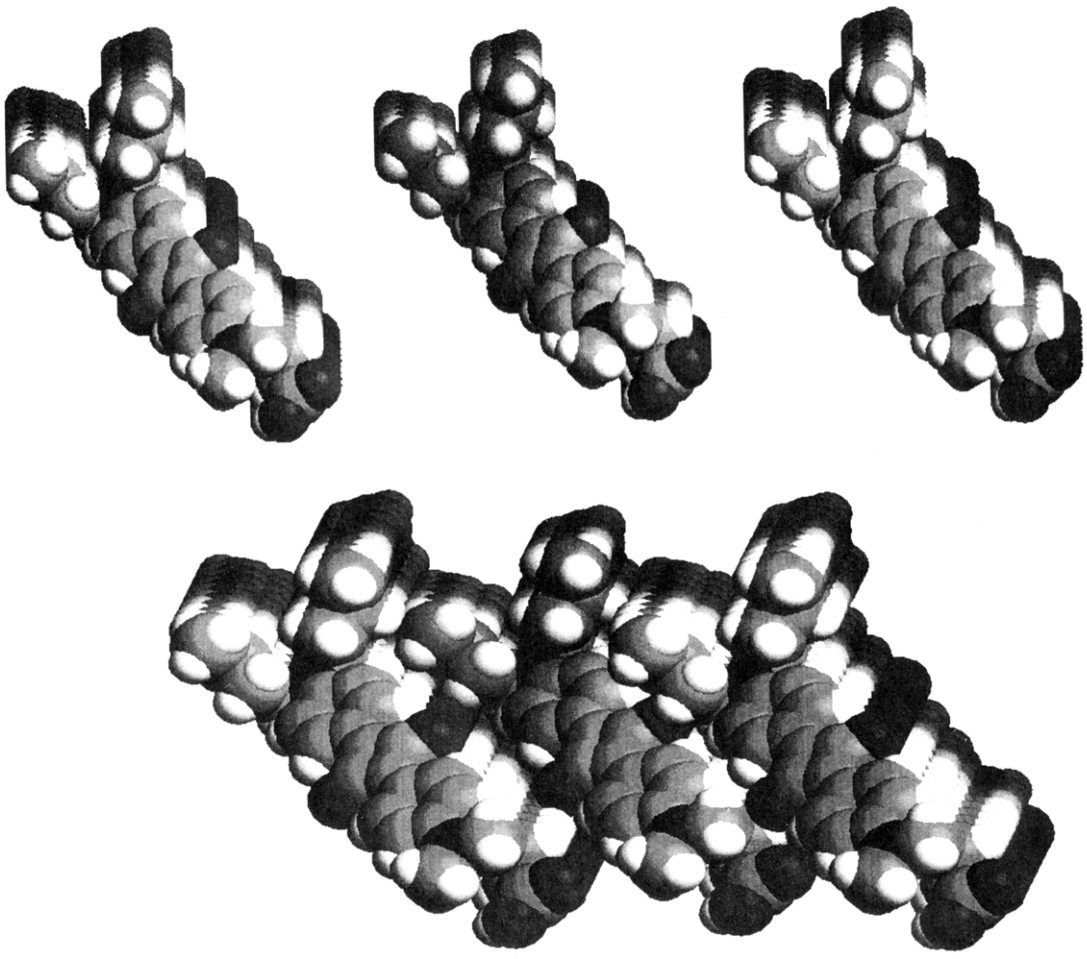

Figure 10. Monte Carlo simulation results for the apparent global minimum of the translation layer. The top view is a cross section of three identical translation chains slightly tilted to show the stacking down the 4.90-Å *b*-axis. These three chains come together in the bottom view to make the translation layer. The 8.92-Å *a*-axis points to the right. In contrast to the glide layer (Figure 9), the hydrophobic surface (top) is quite open where the hydrophilic surface (bottom) is smoother.

tilt angle of the chromophore unit with respect to the layer (water or support) surface normal, and the energy above the global minimum.

The parameters listed in Table 3 can be compared with the measured experimental parameters from the LB films at the air–water interface and the supported monolayers. For example, the measured area/molecule of 38 Å^2 is quite close to that of local minimum 1 of the glide layer (37.14 Å^2/molecule) and not too much smaller than the global minimum for the translation layer (42.59 Å^2/molecule). On the other hand, the tilt angle measured for freshly prepared supported layers (blue-shifted absorption spectrum) of 50 ± 2° is close to the calculated values for the global minimum and first local minimum for the glide layer structure but higher than most of the translational layer structures; the higher tilt angle measured for heated layers (red-shifted) of SBA (60°) is also more consistent with the values estimated for glide layers. The two calculated structures (shown in cross section in Figures 9 and 10) are quite different. The glide layer (Figure 9) has a very open structure on the hydrophilic side, sufficiently open to accommodate water molecules in the cavities between the hydrophilic groups, whereas the hydrophobic side is very compact. In contrast, the translation layer structure (Figure 10) is just the opposite, with a compact hydrophilic surface and a more open hydrophobic one. While there is certainly not enough evidence available to make a definitive assignment at this time, a reasonable hypothesis might be that the glide layer structure affords the best basis for explaining the influence of water (and heating) on the interconversion of the two aggregated forms observed for the LB assemblies. A "glide dimer" is also a reasonable structure for the dimer observed in water and cyclodextrins in that it minimizes dipole–dipole repulsions while the open structure allows chromophore solvation by water while minimizing the hydrophobic surface that must be solvated. Models also suggest that the "glide dimer" can be accommodated within the cavity of γ-cyclodextrin. It is worth noting that despite the difference in arrangements between the hydrophilic and hydrophobic chains in the glide layer and the translation layer the intermolecular interaction between the squaraine chromophores in these layer structures is quite similar. In fact, the intermolecular interaction between the squaraine chromophores turns out to be similar to that in the microcrystals of bis(4-methoxyphenyl)squaraine, which also exhibits blue-shifted absorption relative to the monomer.[9,10]

Acknowledgment. We are grateful to the National Science Foundation for support of this work as part of the NSF Center for Photoinduced Charge Transfer (CHE-9120001) and to Professor R. M. Leblanc and Ms. L. Shao for obtaining absorption spectra of SBA on water.

References and Notes

(1) Law, K. Y. *Chem. Rev.* **1993**, *93*, 449.
(2) Law, K. Y. *J. Phys. Chem.* **1987**, *91*, 5184.
(3) Kim, Y. S.; Liang, K.; Law, K. Y.; Whitten, D. G. *J. Phys. Chem.* **1994**, *98*, 984–988.
(4) Kamet, P. V.; Das, S.; Thomas, K. G.; George, M. V. *Chem. Phys. Lett.* **1991**, *178*, 75.
(5) Law, K. Y.; Chen, C. C. *J. Phys. Chem.* **1989**, *93*, 2533.
(6) Buncel, E.; Mckerrow, A.; Kazmaier, P. M. *J. Chem. Soc., Chem. Commun.* **1992**, 1242.
(7) Das, S.; Thanulingam, T. L.; Thomas, K. G.; Kamat, P. V.; George, M. V. *J. Phys. Chem.* **1993**, *97*, 13620.

(8) Bernstein, J.; Goldstein, E. *Mol. Cryst. Liq. Cryst.* **1988**, *164*, 213.
(9) Law, K. Y. *J. Phys. Chem.* **1988**, *92*, 4226.
(10) Farnum, D. G.; Neuman, M. A.; Suggs, W. T. *J. Cryst. Mol. Struct.* **1974**, *4*, 199.
(11) Wingard, R. E. *IEEE Ind. Appl.* **1982**, 1251.
(12) Tristani-Kendra, M.; Eckhardt, C. J. *J. Chem. Phys.* **1984**, *81*, 1160.
(13) Das, S.; Kamat, P. V.; De la Barre, B.; Thomas, K. G.; Ajayaghosh, A.; George, M. V. *J. Phys. Chem.* **1992**, *96*, 10327.
(14) Das, S.; Thomas, K. G.; George, M. V.; Kamat, P. V. *J. Chem. Soc., Faraday Trans.* **1992**, *88*, 3419.
(15) Tessier, A.; Munger, G.; Shao, L.; Gallant, J.; Leblanc, R. M. Proceedings Sixth Int'l Conf. Organized Mol. Films, July 4, 1993, Québec, Canada, p 365.
(16) Quina, F.; Zhou, M., unpublished results.
(17) Hope, M. J.; Bally, M. B.; Webb, G.; Cullis, P. R. *Biophys. Acta.* **1985**, *55*, 812.
(18) Desai, R. D. *J. Indian Inst. Sci.* **1924**, *7*, 235.
(19) Wendling, L. A.; Koster, S. K.; Murry, J. E.; West, R. *J. Org. Chem.* **1977**, *42*, 1129.
(20) De Selms, C. D.; Fox, C. J.; Riordan, R. C. *Tetrahedron Lett.* **1970**, 781.
(21) Law, K. Y.; Bailey, F. C. *Can. J. Chem.* **1993**, *71*, 496.
(22) Zachariasse, K. A.; Whitten, D. G. *Chem. Phys. Lett.* **1973**, *22*, 527.
(23) Herkstroeter, W. G.; Martic, P. A.; Farid, S. *J. Am. Chem. Soc.* **1990**, *112*, 3583.
(24) Kabayashi, N.; Osa, T. *Chem. Lett.* **1986**, 421.
(25) Law, K. Y. *J. Phys. Chem.* **1989**, *93*, 5925.
(26) Kawai, T.; Umemura, J.; Takenaka, T. *Langmuir* **1989**, *5*, 1378.
(27) Vandevyer, M.; Barraud, A.; Texier, R.; Maillard, P.; Giannotti, C. *J. Colloid Interface Sci.* **1982**, *85*, 571.
(28) Kuhn, H.; Möbius, D.; Bücher, H. In *Techniques of Chemistry*; Weissberger, A., Rossiter, B. W., Eds.; Wiley: New York, 1972; Vol. 2, Part IIIB, pp 577–702.
(29) Buss, V. *Angew. Chem. Int. Ed. Engl.* **1990**, *30*, 869.
(30) Degani, T.; Willner, I.; Hass, Y. *Chem. Phys. Lett.* **1984**, *104*, 496.
(31) Hirai, H.; Toshima, N.; Uenoyama, S. *Bull. Chem. Soc. Jpn.* **1985**, *58*, 1156.
(32) Kamura, S. O. *Induced Circular Dichroism in Biopolymer-Dye Systems*; Springer-Verlag: New York, 1986; p 37.
(33) We detected only evidence for a 1:1 complex for SBA with β-CD up to a concentration of β-CD = 5×10^{-3} M; Das et al.[14] have reported a 1:2 (squaraine:β-CD) complex with a differently functionalized squaraine.
(34) Farahat, M., unpublished result.
(35) Song, X.; Furman, I.; Geiger, C.; Zhao, X.-M.; Whitten, D. G., unpublished results.
(36) Perlstein, J. *Science*, submitted.
(37) Perlstein, J. *J. Am. Chem. Soc.* **1992**, *114*, 1955.
(38) Perlstein, J. *J. Am. Chem. Soc.* **1994**, *116*, 455.
(39) Allen, F. H.; Kennard, O.; Taylor, R. *Acc. Chem. Res.* **1983**, *16*, 146.
(40) Chem-X is a molecular modeling program developed and distributed by Chemical Design Ltd., 7-Westway, Oxford, OX2 OJB, U.K.
(41) Allinger, N. L. *J. Am. Chem. Soc.* **1977**, *99*, 8127.
(42) Still, W. C. et al. Macromodel V2.5, Department of Chemistry, Columbia University, New York, NY 10027.
(43) Gasteiger, J.; Marsili, M. *Tetrahedron* **1980**, *36*, 3219.